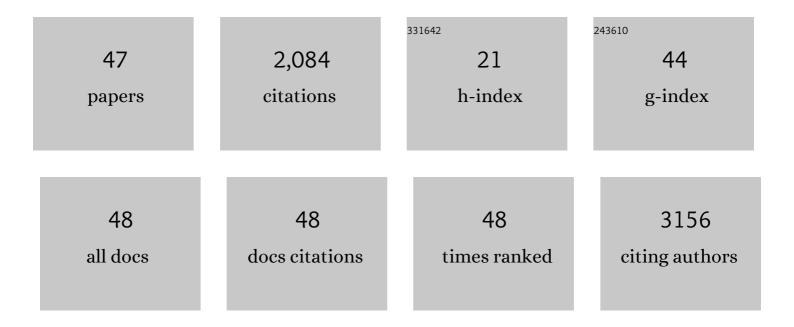
## June-Goo Lee

List of Publications by Year in descending order

Source: https://exaly.com/author-pdf/3056403/publications.pdf

Version: 2024-02-01



LUNE-COOLEE

#	Article	IF	CITATIONS
1	Deep Learning in Medical Imaging: General Overview. Korean Journal of Radiology, 2017, 18, 570.	3.4	834
2	Deep Learning–based Image Conversion of CT Reconstruction Kernels Improves Radiomics Reproducibility for Pulmonary Nodules or Masses. Radiology, 2019, 292, 365-373.	7.3	198
3	CycleMorph: Cycle consistent unsupervised deformable image registration. Medical Image Analysis, 2021, 71, 102036.	11.6	102
4	Improvement of fully automated airway segmentation on volumetric computed tomographic images using a 2.5 dimensional convolutional neural net. Medical Image Analysis, 2019, 51, 13-20.	11.6	75
5	Abdominal multi-organ auto-segmentation using 3D-patch-based deep convolutional neural network. Scientific Reports, 2020, 10, 6204.	3.3	59
6	Fully automated segmentation of cartilage from the MR images of knee using a multiâ€atlas and local structural analysis method. Medical Physics, 2014, 41, 092303.	3.0	49
7	Angiographyâ€Based Machine Learning for Predicting Fractional Flow Reserve in Intermediate Coronary Artery Lesions. Journal of the American Heart Association, 2019, 8, e011685.	3.7	49
8	Deep Learning Algorithm for Reducing CT Slice Thickness: Effect on Reproducibility of Radiomic Features in Lung Cancer. Korean Journal of Radiology, 2019, 20, 1431.	3.4	47
9	Volume Doubling Times of Lung Adenocarcinomas: Correlation with Predominant Histologic Subtypes and Prognosis. Radiology, 2020, 295, 703-712.	7.3	38
10	Development of an Automatic Classification System for Differentiation of Obstructive Lung Disease using HRCT. Journal of Digital Imaging, 2009, 22, 136-148.	2.9	36
11	Machine learning assessment of myocardial ischemia using angiography: Development and retrospective validation. PLoS Medicine, 2018, 15, e1002693.	8.4	34
12	Informatics in Radiology: Dual-Energy Electronic Cleansing for Fecal-Tagging CT Colonography. Radiographics, 2013, 33, 891-912.	3.3	31
13	CT Image Conversion among Different Reconstruction Kernels without a Sinogram by Using a Convolutional Neural Network. Korean Journal of Radiology, 2019, 20, 295.	3.4	30
14	Intravascular ultrasound-based machine learning for predicting fractional flow reserve in intermediate coronary artery lesions. Atherosclerosis, 2020, 292, 171-177.	0.8	30
15	Fully Automatic Coronary Calcium Score Software Empowered by Artificial Intelligence Technology: Validation Study Using Three CT Cohorts. Korean Journal of Radiology, 2021, 22, 1764.	3.4	30
16	Prognostic value of radiomic analysis of iodine overlay maps from dual-energy computed tomography in patients with resectable lung cancer. European Radiology, 2019, 29, 915-923.	4.5	29
17	Machine Learning–Based Automatic Rating for Cardinal Symptoms of Parkinson Disease. Neurology, 2021, 96, e1761-e1769.	1.1	28
18	Performance testing of several classifiers for differentiating obstructive lung diseases based on texture analysis at high-resolution computerized tomography (HRCT). Computer Methods and Programs in Biomedicine, 2009, 93, 206-215.	4.7	27

June-Goo Lee

#	Article	IF	CITATIONS
19	Incremental Value of Subtended Myocardial Mass for Identifying FFR-Verified Ischemia Using QuantitativeÂCT Angiography. JACC: Cardiovascular Imaging, 2019, 12, 707-717.	5.3	26
20	Outcome prediction in resectable lung adenocarcinoma patients: value of CT radiomics. European Radiology, 2020, 30, 4952-4963.	4.5	23
21	Intravascular ultrasound-based deep learning for plaque characterization in coronary artery disease. Atherosclerosis, 2021, 324, 69-75.	0.8	23
22	A straightforward approach to computer-aided polyp detection using a polyp-specific volumetric feature in CT colonography. Computers in Biology and Medicine, 2011, 41, 790-801.	7.0	21
23	Automated detection of vulnerable plaque in intravascular ultrasound images. Medical and Biological Engineering and Computing, 2019, 57, 863-876.	2.8	20
24	MDCT quantification is the dominant parameter in decision-making regarding chest tube drainage for stable patients with traumatic pneumothorax. Computerized Medical Imaging and Graphics, 2012, 36, 375-386.	5.8	19
25	Deep learning–based algorithm to detect primary hepatic malignancy in multiphase CT of patients at high risk for HCC. European Radiology, 2021, 31, 7047-7057.	4.5	19
26	Better Diagnosis of Functionally Significant Intermediate Sized Narrowings Using Intravascular Ultrasound-Minimal Lumen Area and Coronary Computed Tomographic Angiography–Based Myocardial Segmentation. American Journal of Cardiology, 2016, 117, 1282-1288.	1.6	17
27	Automated Segmentation of Left Ventricular Myocardium on Cardiac Computed Tomography Using Deep Learning. Korean Journal of Radiology, 2020, 21, 660.	3.4	17
28	Mathematically Derived Criteria for Detecting Functionally Significant Stenoses Using Coronary Computed Tomographic Angiography–Based Myocardial Segmentation and Intravascular Ultrasound–Measured Minimal Lumen Area. American Journal of Cardiology, 2016, 118, 170-176.	1.6	16
29	Prediction of coronary thin-cap fibroatheroma by intravascular ultrasound-based machine learning. Atherosclerosis, 2019, 288, 168-174.	0.8	16
30	Evaluation of MRI resolution affecting trabecular bone parameters: Determination of acceptable resolution. Magnetic Resonance in Medicine, 2012, 67, 218-225.	3.0	15
31	Novel Methodology to Evaluate Renal Cysts in Polycystic Kidney Disease. American Journal of Nephrology, 2014, 39, 210-217.	3.1	12
32	Impact of Subtended Myocardial Mass Assessed by Coronary Computed Tomographic Angiography-Based Myocardial Segmentation. American Journal of Cardiology, 2019, 123, 757-763.	1.6	12
33	Impact of coronary calcium score and lesion characteristics on the diagnostic performance of machine-learning-based computed tomography-derived fractional flow reserve. European Heart Journal Cardiovascular Imaging, 2021, 22, 998-1006.	1.2	12
34	An Anthropomorphic Phantom Study of Computer-Aided Detection Performance for Polyp Detection on CT Colonography: A Comparison of Commercially and Academically Available Systems. American Journal of Roentgenology, 2009, 193, 445-454.	2.2	10
35	Dual-Energy Index Value of Luminal Air in Fecal-Tagging Computed Tomography Colonography. Journal of Computer Assisted Tomography, 2013, 37, 183-194.	0.9	10
36	Impact of coronary lumen reconstruction on the estimation of endothelial shear stress: in vivo comparison of three-dimensional quantitative coronary angiography and three-dimensional fusion combining optical coherent tomography. European Heart Journal Cardiovascular Imaging, 2018, 19, 1134-1141.	1.2	9

June-Goo Lee

#	Article	IF	CITATIONS
37	Computer-aided polyp detection on CT colonography: Comparison of three systems in a high-risk human population. European Journal of Radiology, 2010, 75, e147-e157.	2.6	8
38	A deep learning–based automatic analysis of cardiovascular borders on chest radiographs of valvular heart disease: development/external validation. European Radiology, 2022, 32, 1558-1569.	4.5	8
39	Hybrid Airway Segmentation Using Multi-Scale Tubular Structure Filters and Texture Analysis on 3D Chest CT Scans. Journal of Digital Imaging, 2019, 32, 779-792.	2.9	7
40	A Portable Smartphone-Based Laryngoscope System for High-Speed Vocal Cord Imaging of Patients With Throat Disorders: Instrument Validation Study. JMIR MHealth and UHealth, 2021, 9, e25816.	3.7	7
41	Association between flow skewness and aortic dilatation in patients with aortic stenosis. International Journal of Cardiovascular Imaging, 2017, 33, 1969-1978.	1.5	6
42	Volumetric assessment of extrusion in medial meniscus posterior root tears through semi-automatic segmentation on 3-tesla magnetic resonance images. Orthopaedics and Traumatology: Surgery and Research, 2020, 106, 963-968.	2.0	6
43	CT Evaluation for Clinical Lung Cancer Staging: Do Multiplanar Measurements Better Reflect Pathologic T-Stage than Axial Measurements?. Korean Journal of Radiology, 2019, 20, 1207.	3.4	6
44	Plaque structural stress assessed by virtual histology-intravascular ultrasound predicts dynamic changes in phenotype and composition of untreated coronary artery lesions. Atherosclerosis, 2016, 254, 85-92.	0.8	5
45	Accuracy of the femoral tunnel position in robotâ€assisted anterior cruciate ligament reconstruction using a magnetic resonance imagingâ€based navigation system: A preliminary report. International Journal of Medical Robotics and Computer Assisted Surgery, 2018, 14, e1933.	2.3	5
46	Intravascular ultrasoundâ€derived morphological predictors of myocardial ischemia assessed by stress myocardial perfusion computed tomography. Catheterization and Cardiovascular Interventions, 2017, 89, E207-E216.	1.7	3
47	An Automated Classification System for the Differentiation of Obstructive Lung Diseases based on the Textural Analysis of HRCT images. Journal of the Korean Radiological Society, 2007, 57, 21.	0.0	0